8. R. Tasker, *Far Eastern Econ. Rev.* **148**, 18 (5 April 1990).
9. L. G. Martin, *Pop. Bull.* **44** (no. 2) (1989).
10. *Scope* (Center for Immigration Studies, Washington, DC) (winter 1990), p. 8.
11. *Far Eastern Econ. Rev.* **145**, 14 (10 August 1989).
12. C. Goldstein, *ibid.* **148**, 49 (14 June 1990).
13. S. J. Hoon, *ibid.* (5 April 1990), p. 19.
14. J. Moore, *ibid.*, p. 20.
15. Private retirement benefits are not discussed here. For a review of Japanese benefits, which include pensions and lump-sum retirement allowances, see R. L. Clark, *Retirement Systems in Japan* (Irwin, Homewood, IL, 1990). This discussion of the Japanese public pension system focuses on its earnings-related component, which covers approximately 45% of the labor force. Starting at age 65, the self-employed, unemployed, and dependent spouses of workers covered by the earnings-related component, plus those workers themselves, also receive a basic public pension that is unrelated to earnings.
16. E. Salem, *Far Eastern Econ. Rev.* **141**, 141 (8 September 1988).
17. A. J. Chen and P. P. L. Cheung, *The Elderly in Singapore* (Ministry of Health, Singapore, 1988).
18. L. G. Martin, *J. Gerontol.* **43**, S99 (1988).
19. How health and productivity will change as life expectancy increases is subject to debate. See, for example, J. F. Fries, *Milbank Q.* **67**, 208 (1989); R. G. Rogers, A. Rogers, A. Belanger, *ibid.*, p. 370; K. G. Manton, *ibid.* (suppl., part 2), p. 13.
20. Japan Statistics Bureau, *Annual Report on the Labor Force Survey 1987* (Tokyo, 1988), pp. 23 and 27; U.S. Bureau of Labor Statistics, *Employment Earnings* **35**, 160 (1988).
21. R. V. Burkhauser and J. F. Quinn, *Res. Labor Econ.*, in press.
22. A. Seike, "The effect of employees pension on the labor supply of the Japanese elderly," *Rand Note, No. 2862* (1989).
23. Japan Ministry of Labor, *Employment and Management Survey* (Tokyo, 1987).
24. J. H. Schulz, K. Takada, S. Hoshino, *When "Lifetime Employment" Ends: Older Worker Programs in Japan* (Policy Center on Aging, Brandeis University, Waltham, MA, 1989).
25. The largest U.S. employment program specifically designed for the elderly is the Department of Labor's Senior Community Service Employment Program (Title V, Older Americans Act), which in 1989 allocated $344 million to states and nonprofit organizations to create jobs for low-income persons 55 and over [Office of Information *News 89-376* (U.S. Department of Labor, Washington, DC, 1 August 1989)].
26. Japan Management and Coordination Agency, *Report on the International Comparative Survey on the Lives and Perceptions of the Elderly* (Tokyo, 1987, in Japanese).
27. M. Osako, *Prod. Aging News* **25**, 1 (July–August 1988).
28. N. Maeda, in *Caring for an Aging World*, T. Schwab, Ed. (McGraw-Hill, New York, 1989), p. 253; National Center for Health Statistics, *Health Statistics on Older Persons, U.S., 1986* (Department of Health and Human Services, Hyattsville, MD, 1987), pp. 64–65.
29. R. N. Butler and M. M. Osako, *Washington Post*, 5 June 1990, p. 6.
30. K. H. Phua, *World Health Forum* **8**, 38 (1987).
31. J. Liang and S. Gu, in *Caring for an Aging World*, T. Schwab, Ed. (McGraw-Hill, New York, 1989), p. 278.
32. L. G. Martin, *Ann. Am. Acad. Polit. Soc. Sci.* **510**, 102 (1990).
33. N. Ogawa, in *Economic and Social Implications of Population Aging* (United Nations, New York, 1988), p. 272.
34. United Nations, *World Population Prospects 1988* (United Nation, New York, 1989).

Ultrafast X-ray Pulses from Laser-Produced Plasmas

MARGARET M. MURNANE,* HENRY C. KAPTEYN,* MORDECAI D. ROSEN, ROGER W. FALCONE

A high-temperature plasma is created when an intense laser pulse is focused onto the surface of a solid. An ultrafast pulse of x-ray radiation is emitted from such a plasma when the laser pulse length is less than a picosecond. A high-speed streak camera detector was used to determine the duration of these x-ray pulses, and computer simulations of the plasmas agree with the experimental results. Scaling laws predict that brighter and more efficient x-ray sources will be obtained by the use of more intense laser pulses. These sources can be used for time-resolved x-ray scattering studies and for the development of x-ray lasers.

DURING THE LAST 20 YEARS THERE HAS BEEN GREAT progress in the development of subpicosecond laser sources at infrared, visible, and ultraviolet wavelengths (*1*). Recently, ultrafast x-ray sources have been demonstrated; this development is based on emission from high-density, laser-produced plasmas (*2–4*). X-rays from these sources are incoherent but have high brightness as a result of the small size, short lifetime, and high temperature of the radiating plasma. Pulses with a duration of a picosecond or less have been observed, more than an order of magnitude shorter than those produced by any other x-ray source. Experimental demonstration of ultrafast x-ray sources was made possible by the development of high-power, ultrashort pulse lasers (*5, 6*) and by improvements in the time resolution of picosecond x-ray detectors (*7*). The applications of such fast x-ray sources and detectors include time-resolved x-ray scattering of rapidly evolving materials (such as diffraction from structures undergoing rapid phase transitions) (*8*), time-resolved photoemission (*9*), and flashlamp pumping of x-ray lasers (*4, 10*).

When a solid is illuminated by intense laser light, electrons in the material absorb energy and are rapidly heated. Hot electrons can subsequently ionize the much cooler atoms, forming an x-ray–emitting, high-temperature plasma spark at the surface of the solid. Laser-produced plasmas have been investigated since the 1960s in inertial-confinement fusion studies (*11*), and recently they have been used as a medium for x-ray lasers (*12*). Incoherent x-ray emission from plasmas has long been recognized as a useful laboratory light source and has been used for time-resolved absorption measurements (*13*), photopumping short-wavelength lasers (*14*), x-ray microscopy (*15*), and x-ray lithography (*16*). A general comparison of laser-produced plasmas with other x-ray sources is difficult because of specific system requirements. However, it is generally true that laser-produced plasmas yield x-rays with much higher peak power but lower average power than do synchrotrons and other high–average power sources such as rotating anode tubes.

Plasmas produced by short laser pulses are fundamentally different from plasmas produced by long laser pulses (*17, 18*). Laser pulses with a duration of 1 ps or more allow significant expansion of the

M. M. Murnane, H. C. Kapteyn, and R. W. Falcone are in the Department of Physics, University of California at Berkeley, CA 94720. M. D. Rosen is at the Lawrence Livermore National Laboratory, Livermore, CA 94550.

*Present address: Department of Physics, Washington State University, Pullman, WA 99164.

plasma into the surrounding vacuum on a time scale shorter than the duration of the laser pulse. A density gradient then forms above the surface of the solid. Laser light is absorbed in this gradient at a density at which the electron plasma frequency equals the laser frequency. This density, the so-called critical density, is typically about 1% of the solid density (*19*). In contrast, for sufficiently short-duration laser pulses, the density gradient that forms is shorter than the penetration depth (skin depth) of the laser field (*20*). Because expansion of the plasma proceeds at the local sound speed of about 0.1 nm fs^{-1} (*19*) and a typical optical skin depth in a metallic solid is 10 nm, laser energy will be deposited in the solid if the laser pulse duration is on the order of 100 fs or less.

Deposition of laser energy at high densities is crucial for the production of short x-ray pulses. Electron heating and the rise time of the emitted x-ray pulse will be comparable to the laser pulse duration. Short x-ray pulses are therefore expected if the plasma can cool rapidly. Deposition of laser energy at solid density allows rapid cooling because (i) the associated high thermal gradient allows rapid conduction of electron energy into the bulk of the solid beyond the optical skin depth; (ii) the associated high pressure gradient allows rapid cooling by expansion into the vacuum in front of the surface; and (iii) nonequilibrium conditions in the underionized plasma allow hot electrons to cool rapidly by inelastic collisions with atoms and ions.

Some of the basic concepts associated with high-density plasmas formed at the surface of solids were discussed more than 20 years ago by Caruso and Gratton (*18*). They predicted the lifetime of a high-temperature, solid-density plasma by equating the scale length of diffusive heat conduction into the solid with the scale length of plasma expansion into the vacuum. This analysis overestimates the actual laser-pulse duration required to create a solid-density plasma; experimental demonstration of the concept had to wait a generation for the development of high-power subpicosecond laser sources.

Experiments with Ultrashort Laser Pulses

Demonstration of short-pulse x-ray emission required the development of two experimental tools. First, a high-power, ultrashort pulse laser system with low prepulse energy was needed as an excitation source. Low prepulse energy or, equivalently, a sharp leading temporal edge is essential because energy deposited in advance of the main pulse can ablate target material and form an opaque vapor, in front of the solid, that will absorb laser energy. Second, an x-ray detector with picosecond time resolution was required.

The laser system used for our experiments (*6*) includes a colliding-pulse, mode-locked laser oscillator, which produces low-energy, 100-fs pulses at a wavelength of 616 nm and a repetition rate of 100 MHz. Selected pulses are amplified at a repetition rate of 10 Hz in a series of five dye-laser amplifiers pumped by two frequency-doubled Nd:YAG (neodymium yttrium-aluminum-garnet) lasers. Amplified pulses with an energy of 5 mJ and a pulse length of 160 fs were directed into a vacuum chamber and focused onto a solid target at power densities up to 10^{16} W cm^{-2}. A scanning stage moved fresh target material into the laser focus for each shot.

The x-ray detector (*3, 7*) consists of a modified commercial x-ray streak camera, with its output phosphor screen imaged onto a sensitive charge-coupled-device (CCD) camera. Streaked images are transferred to a minicomputer for digital storage and analysis. High temporal resolution is obtained by the use of a photocathode with narrow photoelectron energy distribution, a high field to accelerate the emitted electrons, and a fast, well-calibrated sweep speed. A typical data trace of a short x-ray pulse is shown in Fig. 1. A single-shot measurement was made of the relative intensity versus time of broadband soft x-rays from an Si target with photon energy between 50 and 1000 eV. The 2.0-ps x-ray pulse is bracketed by two timing fiducials that were created by frequency doubling a fraction of the ultrashort laser pulse, splitting it into two pulses of known time separation, and directing these pulses onto the photocathode in near coincidence with the x-rays. The frequency-doubled laser light has a pulse duration of less than 300 fs; the observed fiducial pulse duration of 1.6 ps is therefore a first approximation of the instrument response. The calculated response, based on the particular photocathode and camera geometry used, is 1.7 ps. The instrument response can be deconvolved from the measured x-ray pulse duration to yield an upper bound on the x-ray pulse duration of 1.1 ± 1 ps.

Time resolution of an x-ray streak camera is primarily limited by the energy spread of the secondary photoelectrons emitted from the photocathode (*21*). This energy spread elongates the electron bunch and contributes about 1.5 ps to the instrument responses for the KBr and CsI photocathodes used in these experiments. Further improvements in the time resolution of x-ray streak cameras will require new photocathode materials with narrower secondary electron distributions or novel designs that incorporate electron-energy filtering or low-dispersion electron-focusing geometries. Before our work, the best available x-ray time resolution was 10 to 20 ps (*22–25*).

Some fundamental differences between solid-density, subpicosecond laser plasmas and critical density plasmas were demonstrated in two experiments. In the first experiment, the reflectivity of the target as a function of intensity had very different dependence for long (nanosecond) laser pulses than for ultrashort laser pulses (*2*). For a long pulse laser incident on an Si target, the resulting density gradient allows efficient absorption of the laser light and low (<20%) reflectivity at high intensity. In contrast, for ultrashort laser-produced plasmas, reflectivity rises with increasing intensity and reaches a value greater than 85% at 2×10^3 J cm^{-2} (Fig. 2). The reflection is specular even at the highest intensity, indicating that the target stays optically flat with little ablation of the surface during the laser pulse and in contrast to the observed diffuse reflection of long laser pulses. High reflectivity is consistent with the formation of a high-conductivity plasma at the surface of the target (*2, 26*). In the second experiment, the x-ray pulse duration became significantly longer when prepulse laser energy was incident on the target several nanoseconds before the short pulse (*2*). The x-ray pulse lengthens because of the reduced cooling rates in the low-density plasma formed in front of the solid. This experiment also confirmed the importance of a sharp leading edge on the laser pulse.

Radiation from plasmas is composed of line emission (resulting from bound-bound transitions in ions) and continuum emission from both radiative recombination (free-bound transitions of elec-

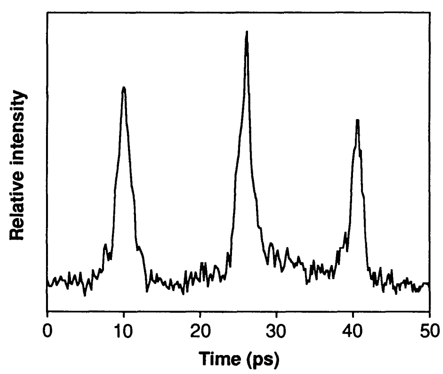

Fig. 1. Streak camera trace of the x-ray emission from an Si target. The x-ray pulse width is 2 ps (full width at half maximum). The x-ray pulse is bracketed by two ultraviolet calibration pulses that are separated by 30 ps.

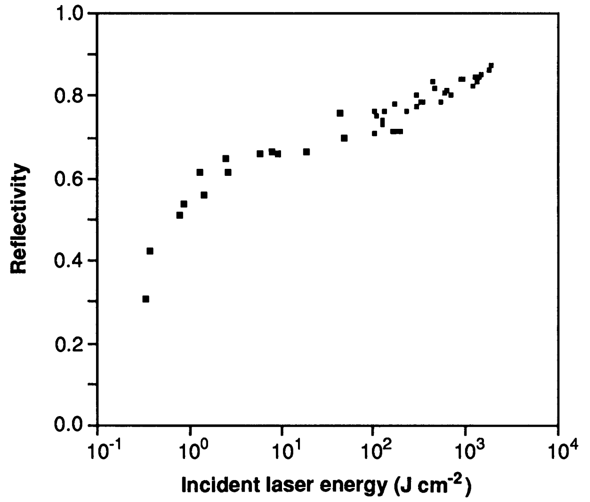

Fig. 2. Reflectivity of a Si target as a function of increasing incident laser energy. The sudden increase in reflectivity indicates a transition from crystalline Si (with a reflectivity of 35%) to molten Si (with a reflectivity of 70%) at the melting threshold.

trons and ions) and bremsstrahlung radiation (free-free transitions of electrons). The time-integrated emission spectrum from the Si target is shown in Fig. 3. At high densities, Stark broadening of line emission and ionization threshold depression are severe and vary rapidly during the evolution of the plasma. Consequently, narrow-line emission will be suppressed at near-solid densities, and broader bandwidth emission will dominate until the plasma expands at later times to lower density. We obtained evidence for long-lived line emission from plasmas by the technique of time-correlated photon counting (TCPC) (*27*), which set a lower limit of 90 ps for the emission on the Ne-like Si transition (n = 3 to 2) at 12 nm. Using TCPC, we found the continuum emission to be instrument-limited at less than 60 ps. The higher resolution streak camera data indicate relatively little radiation (below the detector noise level) later than 2 ps after the laser pulse. We therefore conclude that the long-time-scale line emission contributes little to the total x-ray flux from high-density, short-lived plasmas. The conversion efficiency of laser energy to short-wavelength radiation was measured to be about 0.3% for flat Si targets (*4*).

Models for Solid-Density Plasmas

A simple, damped, free-electron model can be used to calculate the absorption of laser light both in a room-temperature metal and in a high-temperature solid when the electron temperature is well in excess of the Fermi temperature. Electrons within an optical skin depth of the surface absorb energy from the laser field as a result of their relatively low mass and high number density, whereas ions heat relatively slowly by collisions with hot electrons. Screening reduces the intensity of the electromagnetic field in the solid by a factor of $\approx\omega/\omega_p$, where ω is the laser frequency and ω_p is the plasma frequency (*28*). This effect reduces the importance of any high-field or nonlinear absorption mechanisms. During the laser pulse the target material does not expand significantly, and a simple, one-dimensional laser-heating and thermal conduction model (*3, 17*) can be used to predict laser absorption and plasma temperatures. Thermal conductivity in the dense plasma can be several orders of magnitude greater than that of a room-temperature solid (*29*). Ionization equilibrium is approximately valid (at least for low–atomic number targets) because of high collision rates in the dense plasma. Predictions can therefore be made for the ionization stage and electron density as the solid is heated (*30*) and for the peak electron temperature.

Hydrodynamic expansion cooling must be taken into account for more detailed study of the time evolution of the ultrafast laser-heated plasma. In addition, the calculation of the exact electron energy distribution, level populations, and x-ray emission spectrum requires a more complex computer model. We performed calculations (*31*) with the LASNEX simulation code (*32*), which solves nonequilibrium rate equations in the context of an average atom model, along with flux-limited thermal conduction and Lagrangian hydrodynamics. The LASNEX code has been used for 20 years for the simulation of laser-matter interactions with the Inertial Confinement Fusion (ICF) program. Consequently, it has been tested extensively in the regime of 100 ps (and longer) laser pulses, but not in the parameter space discussed in this article. Although ICF plasmas can evolve to a relatively hot, high-density state, our present parameters pose an exciting new challenge to the models in the code, and thus its successful results reported to date (*31*) should be taken with an appropriate amount of caution. The simulation, based on the experimental conditions described above, assumed 30% absorption of the incident laser energy by the Si target in a 10-nm surface layer. Because LASNEX cannot presently predict the absorption due to tunneling into an optical skin depth, we use the code in a post-shot "predictive" mode in which we force the simulation to absorb the measured amount of absorbed laser energy over the duration of the laser pulse.

We performed sensitivity studies to zoning, spatial profiles of deposition layers, local thermodynamic equilibrium (LTE) versus non-LTE, and we used various methods of calculating the electron heat flux under the challenging conditions of very steep gradients. Although the details of those studies are beyond the scope of this review, we present results here for a variety of experiments, using our best guess assumptions. At the peak of the laser pulse, the electron temperature in the plasma is $\approx$500 eV, the electron density is $\approx 7 \times 10^{24}$ cm^{-3}, the ionization state of the silicon is He-like, and the penetration depth of the heat front into the underlying solid is $\approx$60 nm. Only 10% of the available energy has been converted to hydrodynamic motion by this time, and the pressures in the target material can reach 300 Mbar. However, after 2 ps the temperature has dropped to less than 100 eV, and 40% of the energy is now in hydrodynamic motion. The total radiation pulse duration (Fig. 4, curve a) is predicted to be $\approx$800 fs, in reasonable agreement with the experimental data discussed above. Shorter wavelength radiation (Fig. 4, curve b) is expected to be considerably shorter in duration.

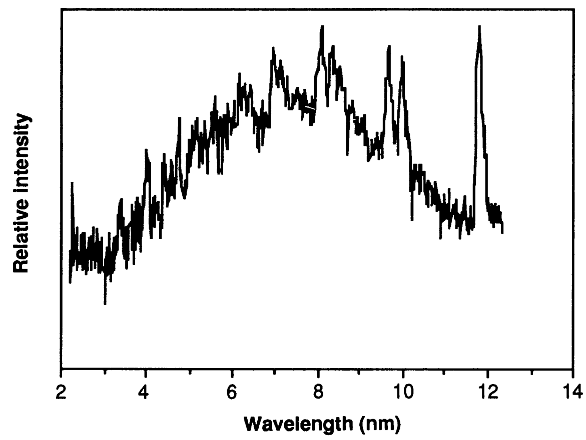

Fig. 3. Time-integrated emission spectrum from an Si target that shows both line and continuum emission.

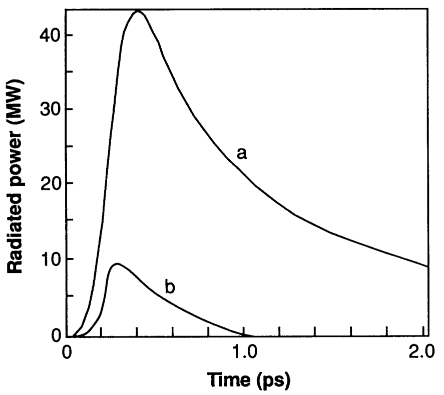

Fig. 4. LASNEX simulation code predictions (curve a) for the total radiation pulse width from an Si target and (curve b) for the pulse width for radiation with energy above 1 keV.

Radiated peak power is estimated to be $\approx 4 \times 10^7$ W, leading to a net energy conversion efficiency of $\approx 0.6\%$ of the incident laser energy, again in reasonable agreement with measurements.

If hydrodynamics are artificially turned off in the simulation, the predicted evolution of the plasma during the laser pulse does not differ significantly from the simulation with the hydrodynamics included. This result is expected, as only 10% of the available energy resides in hydrodynamic motion at this time. However, the two simulations differ at later times, and the predicted output radiation pulse for this no-hydrodynamics case is nearly 2 ps, in disagreement with the experimental results. This analysis points to the importance of the hydrodynamic expansion in the cooling and decompression of the heated target material as a mechanism that leads to faster decay of the radiation pulse.

At much later times (50 to 100 ps after the laser pulse), the simulation predicts that the plasma has cooled to ≈ 25 eV, and part of the original hot solid-density plasma has now expanded to densities of $\approx 10^{21}$ cm^{-3}. A simple hydrogenic atomic model, along with an atomic kinetics simulation code XRASER (*33*), predicts that $\approx 20\%$ of the Si plasma is in the Ne-like state. Predictions for the time history of the Ne-like-Si emission ($n = 3$ to 2) from that plasma indicate a 100-ps time scale, in rough agreement with the TCPC observations described above.

The LASNEX simulations also predict the behavior of the plasma in the presence of a prepulse (here assumed to have a 2-ns duration). The model shows x-ray pulse durations ranging from 2 to 30 ps for prepulse energies of 0.05 to 10% of the main pulse energy. These values compare well with the experimental data (*2*). The predicted emission spectrum from the Si target is also in reasonable agreement with experimental observations.

In addition to complex simulations, simple arguments can be used to derive scaling laws that predict the response of the plasma as laser parameters are varied (*31*). Because hydrodynamic expansion is negligible during the excitation pulse, we can equate the incident heating flux to a cooling flux due to classical thermal conduction and derive expressions for the electron temperature T (in electron volts) and heat-front penetration scale length L (in nanometers):

$$T = 710\, \tau^{2/9}\, I^{4/9} \tag{1}$$

$$L = 68.5\, \tau^{7/9}\, I^{5/9}/Z \tag{2}$$

where τ is the laser pulse length (in units of 100 fs), I is the absorbed power irradiance (in units of 10^{16} W cm^{-2}), and Z is the ionization state (normalized to 13). At later times t, after the laser pulse terminates, hydrodynamic cooling begins to dominate and we have

$$T \propto E^{2/3}/t^{2/3} \tag{3}$$

$$L \propto E^{1/3}\, t^{2/3} \tag{4}$$

where $E = I\tau$ is the absorbed energy in joules per square centimeter.

Scaling laws can also be used to predict radiative output. The very short heat-penetration depth of ≈ 50 nm on the 100-fs time scale causes the hot radiating region to be optically thin. In other words, the radiation Planck mean free path λ is much longer than the scale length L. The system therefore radiates as a diluted black body, with a power P_r given by

$$P_r = A\sigma T^4 L/\lambda \tag{5}$$

where A is the radiating area and σ is the Stephan-Boltzmann constant. Scaling for the radiation mean free path can be estimated (*31*) with LASNEX. It has a different form for low–atomic number emitters with few bound-bound transitions than for high–atomic number emitters. For Si, λ (in centimeters) is given by

$$\lambda \approx 3 \times 10^{-10}\, T^{2.5} \tag{6}$$

(For Yb, LASNEX yields $\lambda \approx 10^{-7}\, T$.) In our Si target experiments, $A \approx 3 \times 10^{-6}$ cm^2, $T \approx 500$ eV, and $L \approx 50$ nm. We then obtain a peak radiated power of 6×10^7 W, approximately consistent with both the measurements and the LASNEX simulations. From Eqs. 1, 2, 5, and 6, the x-ray conversion efficiency is predicted to vary approximately as $E^{2/9}$ for low–atomic number targets and as $E^{8/9}$ for high–atomic number targets. The LASNEX simulations predict dependencies of $E^{0.2}$ and $E^{0.6}$, respectively. From Eqs. 3 to 6, pulse lengths are seen to be on the order of 1 ps, in agreement with measurements and LASNEX simulations.

Related Plasma Experiments

The new regime of plasma physics that can be studied with high-density, short-lived plasmas has yielded many exciting experiments and proposals. For example, a group at AT&T Bell Laboratories (*26*) derived the resistivity of solid Al from room temperature up to approximately 100 eV (10^6 K) by using the measured reflectivity of ultrashort laser pulses. The resistivity initially rose to a broad maximum before decreasing at higher temperatures approaching 100 eV. Resistivity saturation is attributed to a minimum in the electron mean free path when the scattering length corresponds approximately to the interatomic spacing.

Preliminary results have been reported on a novel method of measuring x-ray pulse duration that potentially has subpicosecond resolution (*34*). This technique uses the nonlinear interaction of visible light and x-rays. An intense visible laser pulse is used to Stark-shift atomic energy levels in Kr gas. X-ray absorption near an autoionizing transition in Kr is monitored in the presence of the laser causing the Stark shift. Modulation of the absorption constitutes an x-ray switch at a specific wavelength, with a switching time equal to the laser pulse duration, and allows a cross-correlation of pulsed x-rays with short laser pulses. Results indicate an x-ray pulse duration on the order of 1 ps.

Thin-foil targets have also been investigated at AT&T Bell Laboratories (*35*) in order to generate hotter plasmas than can be obtained with a solid target. The x-ray yield from foils with thicknesses of 10 nm was seen to increase compared with the x-ray yield of thicker targets because of the higher electron temperatures reached by limiting the energy loss to the bulk by thermal diffusion (*36*). An additional advantage of thin targets is seen in the LASNEX simulations, which predict significantly shorter x-ray output pulses for thin foils. For Si, the calculated radiation pulse decreases from 800 fs for bulk targets to 300 fs for the thin foil, because the drop in density that accompanies exploding foils shortens the x-ray output pulse. In addition, for foils sufficiently thick to just burn through during the laser pulse, there is no significant decrease in peak radiated power, indicating that foils are good targets for producing short-duration intense x-ray pulses.

Characteristic x-ray line emission could be a useful source of radiation from laser-heated plasmas because of the possibility of high conversion efficiency into a narrow spectral bandwidth. Harris and Kmetec (37) have proposed using a mixed species target, consisting of a light element doped with a heavy element. The light or low–atomic number element would be fully ionized, contributing electrons that reach high energies under ultrafast laser excitation. These electrons would ionize inner-shell electrons of the heavy or high–atomic number dopant, yielding intense characteristic x-ray line emission with extremely short pulse duration.

Related experiments have been performed with laser pulses having durations from several hundred femtoseconds to several picoseconds (23, 38). Although laser energy was deposited near the critical plasma density because of either prepulse energy or the length of the laser pulse itself, x-ray emission may be observed from dense material in these experiments because of rapid thermal conduction. The advantage of having a prepulse is that the laser energy can be efficiently coupled into critical-density plasma. A group from Los Alamos National Laboratory (24, 39) observed strong emission from He-like lines in a critical-density Al plasma excited by a subpicosecond 308-nm laser. Because the atom is stripped to a stable ionic core, competing Auger decay is reduced, and x-ray conversion efficiency into kiloelectron-volt line radiation approaches 0.5% of the laser energy. The radiative lifetimes of these lines are subpicosecond in duration.

An alternative technique of a short-pulse x-ray generation is under development by Wonterghem and Rentzepis (40). They use an x-ray tube with an unconventional photocathode as an electron source. A short-pulse laser produces an electron burst from the photocathode; these electrons are accelerated into an anode and yield hard x-rays. X-ray pulse durations of less than 70 ps have been obtained by this technique.

Recently, we demonstrated a technique that may be useful in the generation of ultrashort plasmas at higher laser intensities (41). Reflectivity at a sharp plasma interface is very high, and more than 85% of normally incident light was reflected by the target at the highest laser intensity. This effect will result in reduced x-ray yields as even more powerful laser systems are used to heat plasmas. However, we have observed that roughened surfaces generally give higher x-ray yields than do smooth targets. To quantify this effect, we studied x-ray emission and laser reflectivity from targets with well-defined, subwavelength-scale surface structure. The targets were rectangular grooved gratings, with periodicities of 240 and 300 nm and depths ranging from 150 to 200 nm. These grating patterns were produced in Si by optical lithography and chemical etching. For normal incidence illumination, with the laser polarization perpendicular to the grooves of the grating, reflectivity of the structure remained less than 10% for intensities up to 10^{16} W cm^{-2}. An increase in short-pulse x-ray emission by a factor of 12 was also observed, compared with the emission from flat Si targets. This increased x-ray yield is primarily due to the penetration of the laser into the grooved structure, which may increase both the effective laser field and the available surface area of the target.

The high reflectivity of plasmas produced on flat targets may actually be of practical use in the realization of solid-density plasmas at very high intensities. Expansion is much less than the laser wavelength, so that reflected light maintains good optical quality when plasmas are produced by ultrafast laser pulses. We recently demonstrated (41) a method of prepulse energy suppression that relies on this phenomenon. In the experiment, an ultrashort laser pulse preceded by prepulse energy was focused onto an initially transparent glass target. The focused intensity was adjusted so that the prepulse was not sufficient to ionize the target, but the ultrashort pulse created a dense plasma. Prepulse energy passed through the glass target while the short pulse was reflected from a high-density plasma it rapidly created. As a result, the intensity contrast ratio of short-pulse energy to prepulse energy was increased upon reflection from the glass target. We observed that the light reflected off this plasma shutter could be refocused to create an x-ray–emitting plasma and that the intensity of the prepulse is sufficiently reduced so that a solid-density plasma can be created even under conditions of initially high prepulse energy.

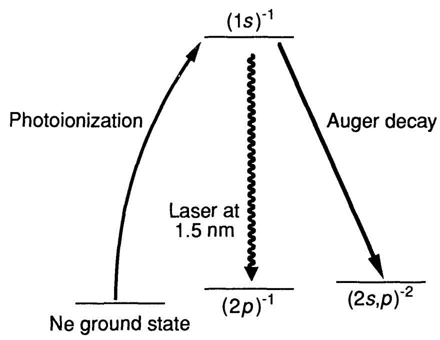

Fig. 5. Energy level diagram for an x-ray laser scheme to produce a population inversion on the Ne K_α x-ray transition at 1.5 nm. Ultrafast x-ray pulses are used as a flash-lamp pump source.

Future Prospects

An important potential application of intense, ultrafast x-ray pulses is an excitation source for short-wavelength lasers (42). We are pursuing a scheme to use such an x-ray flash lamp to create a population inversion on the Ne K_α x-ray transition at 1.5 nm. A diagram of the x-ray laser scheme is shown in Fig. 5. The K_α transition can be populated by x-ray photoionization of inner-shell electrons. Although rapid Auger decay to doubly ionized Ne depopulates the upper laser level and electron collisions fill the lower level, calculations (4, 10) show that a sufficiently intense, short-duration, and spectrally filtered x-ray pump will cause a population inversion in singly ionized Ne. Extrapolating from our current results, we estimate that laser energies between 1 and 10 J in a 50-fs pulse will be needed to produce the required x-ray pump power. The resulting x-ray laser output is expected to have good spatial coherence, an energy of about 10 μJ, and a pulse length of 10 fs. Such an x-ray laser source would make possible a variety of experiments in x-ray nonlinear optics and time-resolved x-ray scattering.

Short-pulse lasers with energies of several joules are being developed at several laboratories (43). The technique of chirped pulse amplification (CPA) (44) is being used to increase the energy of short-pulse lasers by several orders of magnitude. In CPA, a broad-bandwidth, low-energy pulse is temporally stretched (by a factor of up to 10^4) by use of a pair of diffraction gratings, resulting in a long pulse with a frequency that varies linearly as a function of time. This pulse is amplified to high energy (while maintaining low peak power in laser amplifiers) and is then recompressed to ultrafast time scales with another pair of gratings. New laser materials such as Ti-doped sapphire have a sufficiently wide gain spectrum to amplify these pulses and also have high-energy extraction limits (45). Laser systems capable of generating 100-fs pulses with energies of several joules now appear possible. Given the predicted scaling law variation of x-ray conversion efficiency as $E^{8/9}$ in high–atomic number materials, the x-ray yield from plasmas should exceed 10% at an absorbed irradiance in excess of 10^{18} W cm^{-2}.

With the use of new, high-energy, short-pulse lasers and increased x-ray emission from carefully structured targets, the next generation of laser-produced plasma x-ray sources will yield extremely short-duration, high-intensity, and short-wavelength pulses. Such sources will increase the time resolution in experiments involving traditional x-ray scattering techniques. Fast x-ray streak cameras will find application by themselves for high time resolution in experiments that use relatively long-duration x-ray sources such as synchrotrons. In addition, the high-density plasmas produced under subpicosecond illumination can be used to test our understanding of the physics of highly excited solids.

REFERENCES AND NOTES

1. See, for example, C. B. Harris, E. P. Ippen, G. A. Mourou, A. H. Zewail, Eds., *Ultrafast Phenomena VII* (Springer-Verlag, Berlin, 1990).
2. M. M. Murnane, H. C. Kapteyn, R. W. Falcone, *Phys. Rev. Lett.* **62**, 155 (1989).
3. M. M. Murnane, thesis, University of California at Berkeley (1989).
4. ——, H. C. Kapteyn, R. W. Falcone, *IEEE J. Quantum Electron.* **25**, 2417 (1989).
5. R. L. Fork, C. V. Shank, R. T. Yen, *Appl. Phys. Lett.* **41**, 223 (1982).
6. M. M. Murnane and R. W. Falcone, *J. Opt. Soc. Am. B* **5**, 1573 (1988).
7. M. M. Murnane, H. C. Kapteyn, R. W. Falcone, *Appl. Phys. Lett.* **56**, 1948 (1990).
8. D. M. Mills, *Phys. Today* **37**, 22 (April 1984).
9. J. Bokor, *Science* **246**, 1130 (1989).
10. H. C. Kapteyn, thesis, University of California at Berkeley (1989).
11. N. G. Basov *et al.*, *Sov. J. Quantum Electron.* **1**, 2 (1971).
12. D. L. Matthews *et al.*, *Phys. Rev. Lett.* **54**, 110 (1985); M. D. Rosen *et al.*, *ibid.*, p. 106; S. Suckewer, C. H. Skinner, H. Milchberg, C. Keane, D. Voorhees, *ibid.* **55**, 1753 (1985).
13. K. Murakami *et al.*, *ibid.* **56**, 655 (1986).
14. H. C. Kapteyn, R. W. Lee, R. W. Falcone, *ibid.* **57**, 2939 (1986).
15. J. A. Trail and R. L. Byer, *Opt. Lett.* **14**, 539 (1989).
16. P. Gohil *et al.*, *Appl. Opt.* **24**, 2024 (1985).
17. R. W. Falcone and M. M. Murnane, in *Short Wavelength Coherent Radiation: Generation and Applications*, D. T. Attwood and J. Bokor, Eds. (American Institute of Physics, New York, 1986), pp. 81–85.
18. A. Caruso and R. Gratton, *Plasma Phys.* **11**, 839 (1969).
19. C. E. Max, in *Les Houches, Session XXXIV, 1980—Interaction Laser-Plasma*, R. Balian and J. C. Adam, Eds. (North-Holland, Amsterdam, 1982), pp. 301–410.
20. O. L. Landen, D. G. Stearns, E. M. Campbell, *Phys. Rev. Lett.* **63**, 1475 (1989); J. C. Kieffer *et al.*, *ibid.* **62**, 760 (1989); J. C. Kieffer *et al.*, *IEEE J. Quantum Electron.* **25**, 2640 (1989); H. M. Milchberg and R. R. Freeman, *J. Opt. Soc. Am. B* **6**, 1351 (1989); R. Fedosejevs *et al.*, *Phys. Rev. Lett.* **64**, 1250 (1990); R. Fedosejevs *et al.*, *Appl. Phys. B* **50**, 79 (1990).
21. B. L. Henke, J. Liesegang, S. D. Smith, *Phys. Rev. B* **19**, 3004 (1979).
22. D. J. Bradley *et al.*, *Opt. Commun.* **15**, 231 (1975).
23. O. Willi, G. Kiehn, J. Edwards, V. Barrow, R. Smith, in *Short Wavelength Coherent Radiation: Generation and Applications*, R. W. Falcone and J. Kirz, Eds. (American Institute of Physics, New York, 1989), pp. 194–199; D. G. Stearns, O. L. Landen, E. M. Campbell, J. H. Scofield, *Phys. Rev. A* **37**, 1684 (1988).
24. J. A. Cobble *et al.*, *Phys. Rev. A* **39**, 454 (1989).
25. O. R. Wood II *et al.*, *Appl. Phys. Lett.* **53**, 654 (1988).
26. H. M. Milchberg, R. R. Freeman, S. C. Davey, R. M. More, *Phys. Rev. Lett.* **61**, 2364 (1988).
27. H. C. Kapteyn, M. M. Murnane, R. W. Falcone, *Opt. Lett.* **12**, 663 (1987).
28. W. K. H. Panofsky and M. Phillips, *Classical Electricity and Magnetism* (Addison-Wesley, London, 1978).
29. L. Spitzer, *Physics of Fully Ionized Gases* (Interscience, New York, 1962).
30. R. M. More, Z. Zinamon, K. H. Warren, R. Falcone, M. Murnane, *J. Phys.* **49**, C7 (1988); R. M. More, in *Atoms in Unusual Situations* (NATO Advanced Study Institute, Cargese, Italy, January 1986); Y. T. Lee and R. M. More, *Phys. Fluids* **27**, 1273 (1984).
31. M. D. Rosen, in *Femtosecond to Nanosecond High-Intensity Lasers and Applications*, E. M. Campbell, Ed. [Society of Photo-Optical Instrumentation Engineers (SPIE), Bellingham, WA, 1990], pp. 160–169.
32. G. B. Zimmerman and W. L. Kruer, *Comments Plasma Phys.* **2**, 51 (1975).
33. P. L. Hagelstein, thesis, Massachusetts Institute of Technology, Cambridge (1981).
34. L. D. Van Woerkom, R. R. Freeman, W. E. Cooke, T. J. McIlrath, in *Femtosecond to Nanosecond High-Intensity Lasers and Applications*, E. M. Campbell, Ed. (SPIE, Bellingham, WA, 1990), p. 159.
35. H. W. K. Tom, O. R. Wood II, G. D. Aumiller, M. D. Rosen, in *Ultrafast Phenomena VII*, C. B. Harris, E. P. Ippen, G. A. Mourou, A. H. Zewail, Eds. (Springer-Verlag, Berlin, 1990), pp. 107–109.
36. H. W. K. Tom and O. R. Wood, *Appl. Phys. Lett.* **54**, 517 (1989).
37. S. E. Harris and J. D. Kmetec, *Phys. Rev. Lett.* **61**, 62 (1988).
38. C. H. Nam *et al.*, *ibid.* **59**, 2427 (1987); D. Kuhlke, U. Herpers, D. von der Linde, *Appl. Phys. Lett.* **50**, 1785 (1987); G. Kuhnle, F. P. Schafer, S. Szatmari, G. D. Tsakiris, *Appl. Phys. B* **47**, 361 (1988); C. H. Nam *et al.*, *ibid.* **50**, 275 (1990).
39. G. T. Schappert *et al.*, in *Atomic Processes in Plasmas*, Y. K. Kim and R. C. Elton, Eds. (American Institute of Physics, New York, 1989), pp. 217–225.
40. B. V. Wonterghem and P. M. Rentzepis, *Appl. Phys. Lett.* **56**, 1005 (1990).
41. H. C. Kapteyn, M. M. Murnane, A. Szoke, A. Hawryluk, R. W. Falcone, in *Ultrafast Phenomena VII*, C. B. Harris, E. P. Ippen, G. A. Mourou, A. H. Zewail, Eds. (Springer-Verlag, Berlin, 1990), pp. 122–124.
42. M. A. Duguay and P. M. Rentzepis, *Appl. Phys. Lett.* **10**, 350 (1967).
43. M. Pessot, J. Squier, G. Mourou, D. J. Harter, *Opt. Lett.* **14**, 797 (1989); H. C. Kapteyn, A. Sullivan, H. Hamster, R. W. Falcone, in *Femtosecond to Nanosecond High-Intensity Lasers and Applications*, E. M. Campbell, Ed. (SPIE, Bellingham, WA, 1990), pp. 75–81; P. Georges, F. Salin, F. Estable, G. Roger, A. Brun, *Ultrafast Phenomena VII*, C. B. Harris, E. P. Ippen, G. A. Mourou, A. H. Zewail, Eds. (Springer-Verlag, Berlin, 1990), pp. 48–50.
44. O. E. Martinez, *IEEE J. Quantum Electron.* **23**, 1385 (1987); P. Maine, D. Strickland, P. Bado, M. Pessot, G. Mourou, *ibid.* **24**, 398 (1988).
45. P. F. Moulton, *J. Opt. Soc. Am. B* **3**, 125 (1986).

46. This work was supported by the U.S. Air Force Office of Scientific Research, the National Science Foundation, and the Department of Energy through Lawrence Livermore National Laboratory. Collaborations with A. Hawryluk of Lawrence Livermore National Laboratory and J. Bokor of AT&T Bell Laboratories in the experiments on structured targets are gratefully acknowledged. M.M.M. was supported by a University of California President's Postdoctoral Fellowship.